# DNA-Directed Alkylating Ligands as Potential Antitumor Agents: Sequence Specificity of Alkylation by Intercalating Aniline Mustards[†]

A. S. Prakash,*,‡,§ William A. Denny,‖ Trudi A. Gourdie,‖ Kisione K. Valu,‖ Paul D. Woodgate,⊥ and Laurence P. G. Wakelin‡,#

Peter MacCallum Cancer Institute, Melbourne, Victoria, Australia, and Cancer Research Laboratory and Chemistry Department, Auckland University, Auckland, New Zealand

ABSTRACT: The sequence preferences for alkylation of a series of novel parasubstituted aniline mustards linked to the DNA-intercalating chromophore 9-aminoacridine by an alkyl chain of variable length were studied by using procedures analogous to Maxam–Gilbert reactions. The compounds alkylate DNA at both guanine and adenine sites. For mustards linked to the acridine by a short alkyl chain through a para O- or S-link group, 5'-GT sequences are the most preferred sites at which $N^7$-guanine alkylation occurs. For analogues with longer chain lengths, the preference of 5'-GT sequences diminishes in favor of $N^7$-adenine alkylation at the complementary 5'-AC sequence. Magnesium ions are shown to selectively inhibit alkylation at the $N^7$ of adenine (in the major groove) by these compounds but not the alkylation at the $N^3$ of adenine (in the minor groove) by the antitumor antibiotic CC-1065. Effects of chromophore variation were also studied by using aniline mustards linked to quinazoline and sterically hindered tert-butyl-9-aminoacridine chromophores. The results demonstrate that in this series of DNA-directed mustards the noncovalent interactions of the carrier chromophores with DNA significantly modify the sequence selectivity of alkylation by the mustard. Relationships between the DNA alkylation patterns of these compounds and their biological activities are discussed.

Alkylating agents derived from aniline mustard (Figure 1) have cytotoxic and antitumor properties, due to their ability to form covalent interstrand cross-links in cellular DNA (Garcia et al., 1988). The experimental antitumor activity of aniline mustard has been known for many years (Ross, 1949), and the compound has found practical use in the clinic (Young et al., 1976). Two aniline mustard derivatives, chlorambucil and melphalan, are still widely used in cancer chemotherapy. Despite their clinical importance, the usefulness of these drugs is limited by several pharmacological deficiencies that result from the intrinsic chemical reactivity of the alkylating function. They have no special affinity for DNA per se and are readily deactivated through reactions with other molecules (e.g., water, proteins and low molecular weight nucleophilic thiols) (Roberts, 1978; Wang & Tew, 1985). Their intermediate hydrolysis products, the monofunctional mustards, form monoadducts with DNA, in ratios possibly as high as 20:1 with respect to diadducts (Brendel & Ruhland, 1984). Such monoadducts are genotoxic, being a possible cause of mutagenic and carcinogenic events. Thus, the nitrogen mustard antitumor agents have relatively low in vivo dose potencies, and their use is associated with long-term genotoxic effects. Finally, tumors develop resistance to alkylating agents by a variety of mechanisms, notably by the elevation of intracellular levels of glutathione (Susukake et al., 1983).

We are interested in the possibility of ameliorating these deficiencies by targeting aniline mustards to DNA, specifically by attaching them to a DNA-intercalating 9-aminoacridine chromophore (Gourdie et al., 1990). By localizing an alkylating agent on DNA in this manner, it may be possible to bring about efficient interstrand cross-linking using less chemically reactive alkylating functions. If so, this approach may provide more efficacious compounds with reduced toxicities and increased resistance to cellular thiols. Previous papers (Kohn et al., 1987; Price et al., 1968; Mattes et al., 1986; Grunberg & Haseltine, 1980) on structurally unrelated mustard derivatives clearly indicate that the mustard moiety has an intrinsic preference for $N^7$ of guanine with the sites of greatest alkylation being runs of contiguous guanines, but relatively weak alkylation at isolated guanines. However, appending an intercalating chromophore to the alkylating function, as in the case of quinacrine mustard (Kohn et al., 1987), modifies this oligoguanine selectivity and causes additional reaction with guanines at 5'-GT sites.

Here we describe our investigation of the DNA-binding properties of the parasubstituted aniline mustards Me, MeO, and MeS and their corresponding intercalating derivatives $(CH_2)_n$, $(CH_2)_nO$, and $(CH_2)_nS$, in which the mustard is covalently linked to 9-aminoacridine, through the same groups ($CH_2$, O, and S) via an alkyl chain of variable length (Figure 1). We studied the sequence selectivity of alkylation of the compounds, using methods analogous to those of the Maxam–Gilbert sequencing technique, as well as the results of helix unwinding and interstrand cross-linking measurements. Varying the nature of the para substituent modulated the chemical reactivity of the aniline mustard, and, for one example, the effect of cross-linking on the alkylating pattern was investigated by using the structurally homologous monofunctional half-mustard, $HM(CH_2)_3$. In addition, we have probed the effect of varying the structure of the DNA-targeting chromophore on alkylation patterns by studying the 3-tert-butyl derivatives of $(CH_2)_3$, $B(CH_2)_3$ (in which 9-
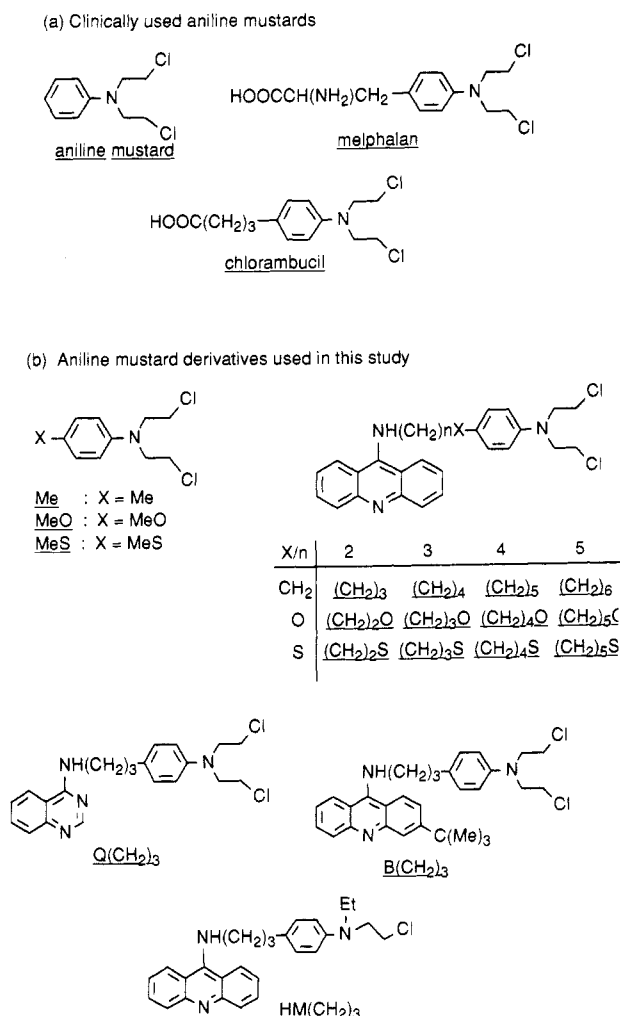
FIGURE 1: Structures of aniline mustard derivatives that are currently in clinical use and the analogues used in this study.

aminoacridine is substituted in the 3-position with a *tert*-butyl group), and another compound, Q(CH$_2$)$_3$, in which the 9-aminoacridine is replaced by the two-ring 4-aminoquinazoline chromophore (Figure 1). We discuss our findings in terms of structure–function relationships and the correlations (if any) which exist between the DNA-binding properties of these compounds and their antitumor activity.

## MATERIALS AND METHODS

Parasubstituted aniline mustards and the corresponding 9-aminoacridine-linked aniline mustards were synthesized as described elsewhere (Gourdie et al., 1990; Valu et al., 1990). The simple aniline mustards are referred to (in terms of their para substituent) as Me, MeO, and MeS, and their intercalating counterparts as (CH$_2$)$_n$, (CH$_2$)$_n$O, and (CH$_2$)$_n$S, where *n* is the number of carbons in the alkyl chain (Figure 1). The antibiotic CC-1065 was a gift from Dr. Bijoy Bhuyan of the Upjohn Co., Kalamazoo, MI. The syntheses of B(CH$_2$)$_3$, Q(CH$_2$)$_3$, and HM(CH$_2$)$_3$, [the half-mustard of (CH$_2$)$_3$] are provided as supplementary material. The compounds are reactive and hydrolyze quite rapidly at room temperature in aqueous solution; thus, they were stored at −20 °C either as solids or as 1 mM solutions in ethanol. Aliquots of stock solutions were diluted to an appropriate concentration in ethanol and added to an aqueous DNA sample to initiate the reaction. The enzymes *Eco*RI, *Bam*HI, Klenow fragment of DNA polymerase I, T4 polynucleotide kinase, and alkaline phosphatase were purchased from Pharmacia. The plasmid pBR322 DNA was obtained from Boehringer-Mannheim.

Other reagents used in this work and their sources are as follows: piperidine, Fluka Chemicals; Tris-HCl and Hepes, Sigma; Na$_2$EDTA, Merck; dimethyl sulfate, Aldrich; ultrapure urea, BRL; sodium chloride and magnesium chloride, Alfa Chemicals. The radioactive nucleotides [$^{32}$P]dATP and [$^{32}$P]ATP were purchased from Bresatec.

*Preparation of $^{32}$P-End-Labeled DNA Fragments.* A 375 base pair *Eco*RI to *Bam*HI fragment of pBR322 DNA was either 3′-end-labeled at the *Eco*RI site by using Klenow fragment and [$^{32}$P]dATP or 5′-end-labeled at the *Eco*RI site by using alkaline phosphatase, T4 polynucleotide kinase, and [$^{32}$P]ATP, according to the published procedures (Maxam & Gilbert, 1980). The fragment was isolated on a 4% nondenaturing polyacrylamide gel. Given below is a partial sequence of the pBR322 DNA used in this work:

```
³¹GCTTTAATGC GGTAGTTTAT CACAGTTAAA TTGCTAACGC ACTCAGGCAC
  CGAAATTACG CCATCAAATA GTGTCAATTT AACGATTGCG TCAGTCCGTG

⁸¹CGTGTATGAA ATCTAACAAT GCGCTCATCG TCATCCTCGG CACCGTCACC
  GCACATACTT TAGATTGTTA CGCGAGTAGC AGTAGGAGCC GTGGCAGTGG

¹³¹CTGGATGCTG
   GACCTACGAC.
```

*Alkylation of Labeled DNA.* Labeled DNA (ca. 30 000 cpm) was incubated with the alkylating agent in the presence of 1 μg of calf thymus DNA in 100 μL of 0.01 SHE buffer (2 mM Hepes, 9 mM NaCl, and 10 μM EDTA, pH 7.3, ionic strength 0.01) at 37 °C for 30 min. The drug to base pair ratio was adjusted against the carrier DNA to obtain not more than one alkylation per labeled fragment for each compound. For compounds (CH$_2$)$_n$, (CH$_2$)$_n$O, Q(CH$_2$)$_2$, and B(CH$_2$)$_2$, a drug to base pair of 0.02 was used. For the simple mustards and the (CH$_2$)$_n$S series, ratios of 0.40 and 0.20, respectively, were required to produce similar levels of strand breaks. The extent of alkylation for each series was determined by taking the natural log ratio of the intensities of the unmodified DNA bands for samples treated with and without the drug.

Time-controlled (1, 5, 10, 20, and 30 min) experiments were also carried out to ensure that the alkylation reached the maximum level well within the incubation period used in the protocol. For experiments with Mg$^{2+}$, the reactions were carried out in the presence of either 30 mM NaCl or 10 mM MgCl$_2$ (final buffer ionic strength 0.04). Preliminary investigations with various concentrations of magnesium ion (1, 5, 10, and 20 mM) showed that the effect of the divalent cation on the alkylation patterns of the mustards under study is negligible at 1 mM and reaches a maximum by about 10 mM. The reaction mixture was chilled in ice, and the modified DNA was precipitated with ethanol and lyophilized.

Two different treatments were used to induce strand breaks at the alkylated sites of DNA. In one treatment (A), the sample was heated in 1 M piperidine (pH 12.5), inducing cleavage primarily at N$^7$ of guanines (Kohn et al., 1987). In the other treatment (B), the sample was heated first in a neutral pH buffer and then in 1 M piperidine. This treatment leads to depurination and subsequent strand breaks at all purines alkylated at N$^7$(G), N$^3$(A), and N$^7$(A) sites (Price et al., 1968; Mattes et al., 1986; Maxam & Gilbert, 1977). The modified DNA pellet was dissolved either in 100 μL of 0.01 SHE buffer (pH 7.3) for treatment B or in 1 M piperidine for treatment A and heated for 10 min at 90 °C. For treatment B, the reaction mixture was then precipitated in ethanol, and a further 10-min heat treatment at 90 °C in 100 μL of 1 M piperidine was carried out. The samples from both treatments were then lyophilized overnight, dissolved in 15 μL of distilled water, and lyophilized again; the last step was repeated once. The dry pellets were then dissolved in a se-

quencing dye made of 80% deionized formamide, 10 mM NaOH, 1% xylene cyanol, and 1% bromophenol blue. The samples were denatured at 90 °C for 2 min before, they were loaded on the sequencing gel.

*Polyacrylamide Gel Electrophoresis.* The sequencing reactions were run on a Sequi-Gen kit from Bio-Rad (21 cm × 50 cm) for 2.5 h at a constant 2400 V in a Tris/borate/EDTA (89 mM/89 mM/2.5 mM, pH 8.3) buffer (TBE) by using a 0.4 mm thick 8% polyacrylamide gel (19:1) containing 8 M urea. The gel was then transferred to a 3-mm Whatman filter paper, covered with plastic wrap, and dried in a Bio-Rad gel drier Model 1125B for 30 min at 80 °C. The gel was then placed in intimate contact with Kodak XAR-5 film and exposed for 10–15 h at −70 °C in the presence of a Du Pont intensifier screen before developing. The densitometer scans were performed on a Zeineh soft laser scanning densitometer (Model SLR -2D/1D- DNA).

*Cross-Linking Measurements.* Cross-linking of DNA by alkylating agents can be conveniently detected on a nondenaturing agarose gel, making use of the fact that the native form of DNA migrates at a slower rate than the denatured form. Cross-linked DNA renatures quickly, and hence the band corresponding to the cross-linked DNA will comigrate with control native DNA. A 3′-end-labeled *Eco*RI digested linear pBR322 DNA fragment was incubated with various concentrations of appropriate agent in the presence of 1 μg of supercoiled pBR322 DNA for 0.5 h at 37 °C. The alkylated DNA was then precipitated in ethanol and dissolved in 10 μL of 0.01 SHE buffer and 2 μL of 1% bromophenol blue dye. Two untreated DNA samples containing no drug were subjected to identical treatment for use as native and denatured DNA controls. The alkylated DNA samples and the control representing denatured DNA were then thermally denatured by heating at 90 °C for 1 min before they were loaded on a nondenaturing 1 cm thick and 10 cm long 1% agarose minigel along with the native DNA control. The samples were run for 90 min in a Tris–phosphate buffer (89 mM Tris base, 2 mM EDTA, and 8.5% phosphoric acid, pH 8.2) at 80 V. The gel was transferred to a 3-mm Bio-Rad filter paper, covered with a plastic wrap, and dried at 80 °C for 1 h. It was then placed in intimate contact with a Kodak XAR-5 film for 15 min in the presence of two Du Pont intensifier screens before developing.

*Helix Unwinding Measurements.* If the alkylating agent, after covalently linking to a supercoiled plasmid DNA, exists in an intercalated orientation, it will lead to unwinding of the supercoil. The extent of unwinding depends on the degree of intercalation as well as the number of such intercalation sites. Since the electrophoretic mobility of a plasmid DNA depends on the extent of supercoiling present, evidence for the intercalative form of the drug can be obtained on a nondenaturating agarose gel by comparing the electrophoretic mobility of the control supercoiled plasmid against the alkylated plasmid. One microgram of supercoiled pBR322 plasmid DNA in 0.01 SHE buffer was incubated with 1 μL of ethanol solution of the alkylating agent at drug to base pair ratios of 0.00, 0.10, 0.15, 0.20, 0.25, 0.30, 0.35, and 0.40 at 37 °C for 30 min in a total number of 10 μL. [Preliminary investigations had shown that reaction mixtures containing final ethanol concentrations of 10% and 2%, respectively, gave identical unwinding results for $(CH_2)_3$.] Two microliters of 1% bromophenol blue dye was added at the end, and the samples were then loaded on a nondenaturing 1 cm thick 1% agarose minigel. (Noncovalently bound drug molecules will quickly move out of the gel and hence play no role in the unwinding of the plasmid.) The
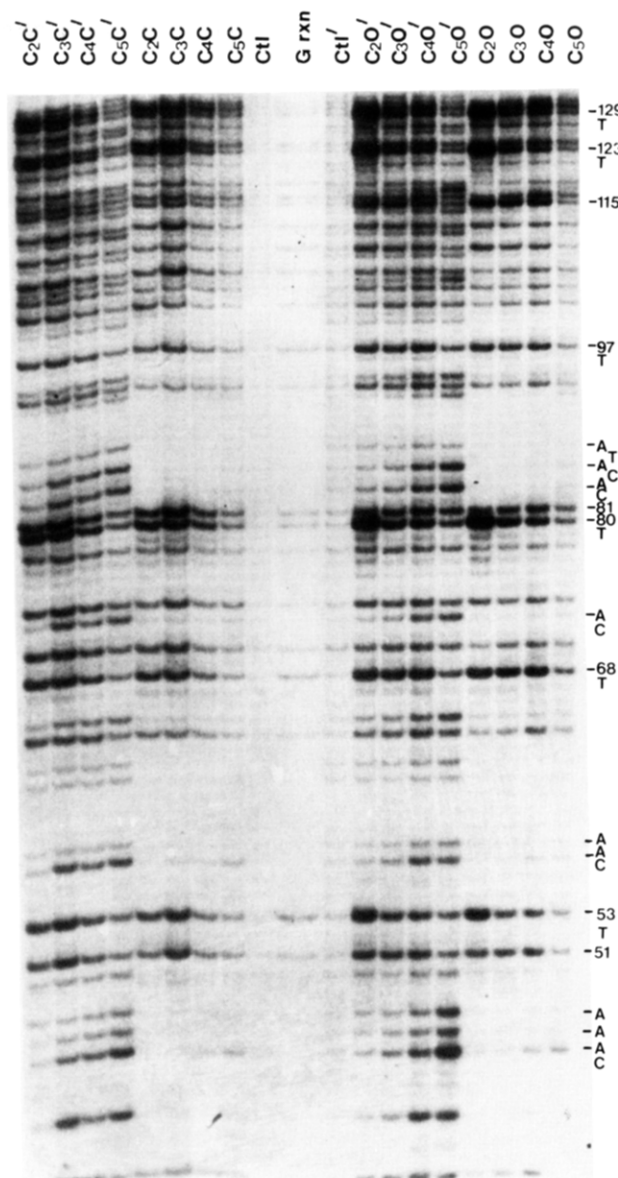


FIGURE 2: Strand cleavage patterns obtained by the chemical treatment of the 3′-end-labeled *Eco*RI to *Bam*HI fragment of pBR322 DNA fragment. The DNA was treated with the homologous series $(CH_2)_n$ (designated $C_nC$; left panel) or the series $(CH_2)_nO$ (designated $C_nO$; right panel) at drug to base pair ratio of 0.02. Letter codes followed by a prime correspond to treatment B, while those without a prime were subjected to treatment A (see text for details). Ctl and Ctl are control DNA samples subjected to treatments A and B, respectively. Lane G rxn corresponds to the Maxam–Gilbert G reaction.

samples were run for 90 min in TP buffer at 80 V. The gel was then stained with ethidium bromide, and the resulting pattern was photographed.

## RESULTS

*Alkylation Pattern of 9-Aminoacridine-Linked Aniline Mustards Using 3′-End-Labeled Fragments. Treatment A.* Lanes labeled with unprimed letter codes in each of the left and right panels of Figure 2 show the strand cleavage patterns of the 3′-end-labeled *Eco*RI/*Bam*HI 375 base pair fragment reacted with compounds from the carbon and oxygen series by using treatment A. For $(CH_2)_n$ compounds, bands corresponding to all Gs are observed, with a slightly greater preference for runs of Gs. The intensity of guanine bands diminishes as the homologous series is ascended. On the other hand, in the $(CH_2)_nO$ series, the most intense bands are ob-

served for guanines at 5'-GT sequences [for $(CH_2)_2O$, bands 53, 68, 80, 97, 123 and 129], the intensities decreasing markedly for compounds of longer chain lengths. The band intensities for guanines in *other* sequences remain weak and nearly constant across the series.

*Treatment B.* Heat treatment at neutral pH followed by further heat treatment in the presence of 1 M piperidine revealed new bands, corresponding to adenines, for all compounds. The intensities of these depended on the DNA sequence as well as on the chain length of these drugs (lanes labeled with primed letter codes in Figure 2); the intensities of the G bands, however, remained essentially the same as those observed in the first treatment. Among adenine bands, 5'-AC sequences were the most preferred, and the intensity of these bands increased with increasing chain length within each series (bands 46, 56, 73, 83, and 85). Thus, there seems to exist an inverse relationship between the band intensities of GT and the complementary AC sequences within a series. The other adenine bands are relatively weak and remain constant with increasing alkyl chain length. The band pattern of the $(CH_2)_nS$ sulfur series is similar to that of the $(CH_2)_nO$ series (gel photos not shown). The top panel in Figure 3 shows the densitometer scans of the band pattern obtained for the $(CH_2)_nS$ compounds by using treatment B. Middle and bottom panels in Figure 3 show densitometer scans of representative compounds from each series—$(CH_2)_3$, $(CH_2)_2O$, and $(CH_2)_2S$.

Band patterns within the $(CH_2)_nS$ series (top panel) demonstrate the inverse relationship displayed by the members of this series for preference between guanine in GT sequences and adenine in AC sequences. It is also clear from Figure 3 (middle panel) that the $(CH_2)_2S$ compound shows the maximum preference for GT sequences of all the compounds studied, and in fact all the bands for this molecule correspond to the trinucleotide sequence, 5'-GTPu (bands 53, 80, 123, and 129). At the other extreme, when the chain length is increased, all three series show a similar general level of complexity in band distribution and, in particular, increased band intensities corresponding to adenines in AC sequences (bottom panel, Figure 3).

*Alkylation Pattern of Simple Aniline Mustards Using 3'-End-Labeled Fragments.* Treatment B revealed a band distribution that was essentially the same for all simple mustards but markedly different from their intercalator-linked derivatives. The densitometer scans for compounds MeO and $(CH_2)_5O$ are shown in the top panel of Figure 4. For MeO, all the guanines show peaks of similar intensity. In addition, peaks corresponding to adenines occurring in runs of adenines (bands 46–48, 56–57, and 61–62) and in 5'-TTA sequences (bands 65 and 94) are observed.

*Effects of Chromophore Variation on Alkylation Pattern of the $(CH_2)_3$-Linked Mustards.* The alkylation patterns of the aniline mustard linked by a $(CH_2)_3$ alkyl chain to quinazoline or to 3-*tert*-butyl-9-aminoacridine chromophores, compounds $Q(CH_2)_3$ and $B(CH_2)_3$, respectively, were obtained to study the effects of noncovalent interactions with DNA on the alkylation pattern. The densitometer scans of $B(CH_2)_3$ and $Q(CH_2)_3$ are shown in the bottom panel of Figure 4 along with that of compound $(CH_2)_3$ for comparison. Compound $B(CH_2)_3$, with the bulky *tert*-butyl group at the 3-position of the 9-aminoacridine chromophore, which prevents intercalation, gives rise to strand breaks at guanines occurring at 5'-GT sequences and in runs of guanines (bands 53, 80, 81, 123, 124, and 129–131). The overall alkylation level is reduced compared to that of the parent compound $(CH_2)_3$. For the
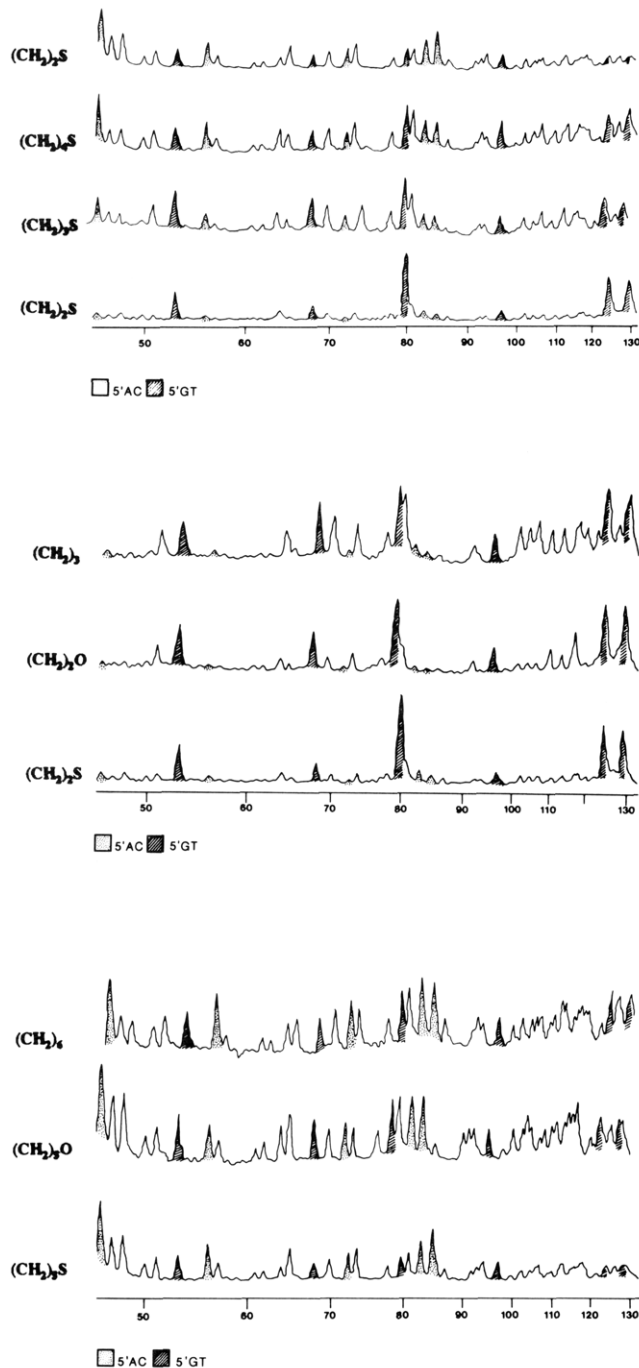


FIGURE 3: (Top panel) Densitometer scans from 3'-end-labeled DNA incubated with the $(CH_2)_nS$ homologues and subjected to treatment B. The scans are normalized with respect to the most intense band [peak 80 of $(CH_2)_2S$] on the autoradiograph to facilitate direct comparison of peak intensities between lanes. (Middle panel) Densitometer scans from 3'-end-labeled DNA incubated with compounds from each series with total chain length of three atoms [compounds $(CH_2)_3$, $(CH_2)_2O$, and $(CH_2)_2S$] and subjected to treatment B. Each scan was normalized with respect to the most intense band within each lane. (Bottom panel) Same as the middle panel, except that compounds from each series with a total chain length of six atoms were used [compounds $(CH_2)_6$, $(CH_2)_5O$, and $(CH_2)_5S$].

quinazoline $Q(CH_2)_3$, bands corresponding to guanines show the same pattern as in the case of $(CH_2)_3$, but in addition adenine bands are observed in some (but not all) AC sequences (bands 56, 83, and 85). Again, the overall alkylation level is lower than that for $(CH_2)_3$.

*Kinetics of DNA Alkylation and Hydrolysis of Aniline Mustards.* Kinetics of DNA alkylation by compounds $(CH_2)_2O$, $(CH_2)_2S$, and MeO were investigated by comparing
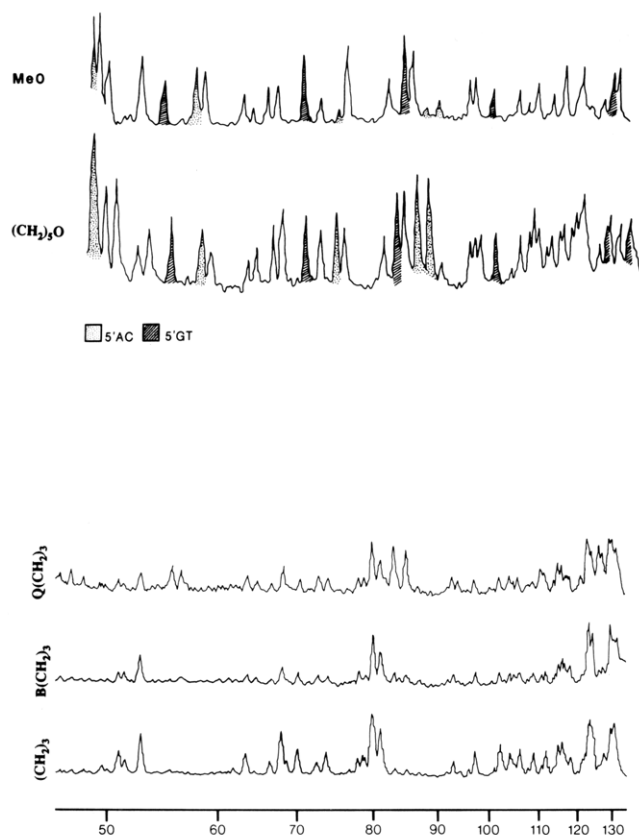
FIGURE 4: (Top panel) Densitometer scans from 3'-end-labeled DNA incubated with compounds $(CH_2)_5O$ and MeO and subjected to treatment B. The drug to base pair ratio is 0.02 for $(CH_2)_5O$ and 0.40 for MeO. (Bottom panel) Densitometer scans of 3'-end-labeled DNA incubated with compounds $(CH_2)_3$, $B(CH_2)_3$, and $Q(CH_2)_3$ and subjected to treatment B. The drug to base pair ratios used are 0.02 for all. The scans are normalized with respect to the most intense band [peak 80 of $(CH_2)_3$] on the autoradiograph.

the band distributions obtained at different incubation times. For all three compounds, there was no change in the band pattern with time; the intensity of the bands reached a maximum within 5 min for $(CH_2)_2O$ and within 10 min for $(CH_2)_2S$ and MeO. The drug to base pair ratio used for $(CH_2)_2O$ was 0.02, which corresponds to about 4 molecules/DNA strand. However, the maximum alkylation at this ratio is only one per labeled strand. The remaining three molecules are hydrolyzed. For $(CH_2)_2S$ and MeO, the ratio of alkylation to hydrolysis is even higher, 1:39 and 1:79, respectively.

*Effects of $Mg^{2+}$ on the Alkylation Pattern of Aniline Mustards.* The left panel in Figure 5 shows the DNA cleavage pattern obtained by using treatment B for compounds $(CH_2)_4O$ and MeO and the antitumor antibiotic CC 1065 (with or without the presence of 10 mM magnesium ion). It has been shown that CC-1065 alkylates adenines occurring at $5'-A_n$ and $5'$-TTA sequences, at the $N^3$ site in the minor groove of DNA (Hurley et al., 1988). For compounds $(CH_2)_4O$ and MeO, band intensities corresponding to As in runs of adenines (bands 33–35, 46–48, 56, 57, 61, and 62) were greatly reduced, while those of all guanines and some isolated adenines (bands 43, 50, 65, 73, and 85) were moderately reduced, when compared to the pattern obtained in the presence of $Na^+$ of similar ionic strength. However, for CC-1065 the intensities of all the adenine bands (bands 33–35, 47, 48, 56, 57, and 94) remained unaffected. At low magnesium ion concentrations (below 1 mM), no detectable change in the band intensities of $(CH_2)_4O$ and MeO were observed (not shown in figure).

*Alkylation Patterns Using 5'-End-Labeled Fragments.* Strand cleavage patterns obtained by using the 5'-labeled 375

base pair fragment showed some interesting features not seen for the 3'-labeled fragment (right panel in Figure 5). The general trend was similar in that the preference for alkylation at GT sequences diminished with increasing $n$, while that for AC sequences increased. In addition, however, the 5'-labeled fragment also showed weak but distinct bands which trailed the strong bands by about 1.5–2 base distance. They are presumably the result of a minor contribution from some unknown cleavage product at the 3'-end of the 5'-labeled fragment. The ghost bands were also observed for the half-mustard $HM(CH_2)_3$, and in fact, the band distribution for the half-mustard is identical with that of the complementary full mustard $(CH_2)_3$ (compare lanes $C_2C'$ and HM in Figure 5, right panel). This indicates that, under the conditions used in this study, DNA cross-linking does not play a role in the observed band pattern for these compounds.

*Cross-Linking and Helix Unwinding Assays.* The cross-linking experiments (Figure 6) show that compounds of the carbon and oxygen series, which are the most reactive alkylating agents, have observable levels of cross-linking even at drug to base pair ratios as low as 0.02, whereas the weaker alkylators (the less reactive compounds in the sulfur series and also the simple mustards) require drug to base pair ratios of 0.40 or above to achieve similar levels of cross-linking. However, even for compounds $(CH_2)_2O$ and $(CH_2)_4O$, at drug to base pair ratio of 0.02, not more than one cross-link has formed per 4362 base pairs of linear pBR322 DNA. This information is obtained by taking the natural log of the fraction of the band intensity of the renatured DNA over that of the total DNA (Mattes et al., 1986). Thus, of a possible 86 molecules of drug available per fragment, only one molecule cross-linked the DNA. At the same input ratio, the kinetic experiments show that there is about one alkylation per 400 bases, or two alkylations per 400 base pairs. Thus, of the 86 drug molecules available per 4362 base pair fragment, 20 alkylation events occur and only 1 leads to cross-linking. For the sulfur species and the simple mustards, the extent of cross-linking is even lower.

Unwinding experiments showed (Figure 7) that only the most reactive of the targeted mustards [the $(CH_2)_nO$ and $(CH_2)_n$ compounds] unwound the helix to any significant extent, leading to loss of right-handed superhelical turns of the plasmid. The results for $(CH_2)_3$ and $(CH_2)_4O$, shown in Figure 7, revealed major differences in the way these two compounds are bound to the plasmid (the results for all the compounds within each series were similar). The compounds in the carbon series $[(CH_2)_n]$ did not completely remove supercoiling, but did induce left-handed superhelical turns above drug to base pair ratio of 0.2. On the other hand, compound $(CH_2)_4O$ (and the other members of the oxygen series) completely removed the right-handed superhelical turns of the plasmid at a drug to base pair ratio of 0.20. However, higher drug concentrations did not induce the left-handed superhelical turns as observed with most nonalkylating intercalators (e.g., ethidium bromide). The weaker alkylators [the $(CH_2)_nS$ series and the simple mustards which lack the intercalating chromophore] did not unwind the superhelix at all, even at a drug to base pair ratio of 0.40.

DISCUSSION

The results presented show that targeting of aniline mustards to DNA by their attachment to DNA-affinic chromophores alters the *pattern* of their alkylation of DNA as well as increases its *degree* severalfold. More unexpectedly, the results also show that such aniline mustards are capable of significant levels of adenine alkylation. Three major conclusions can be
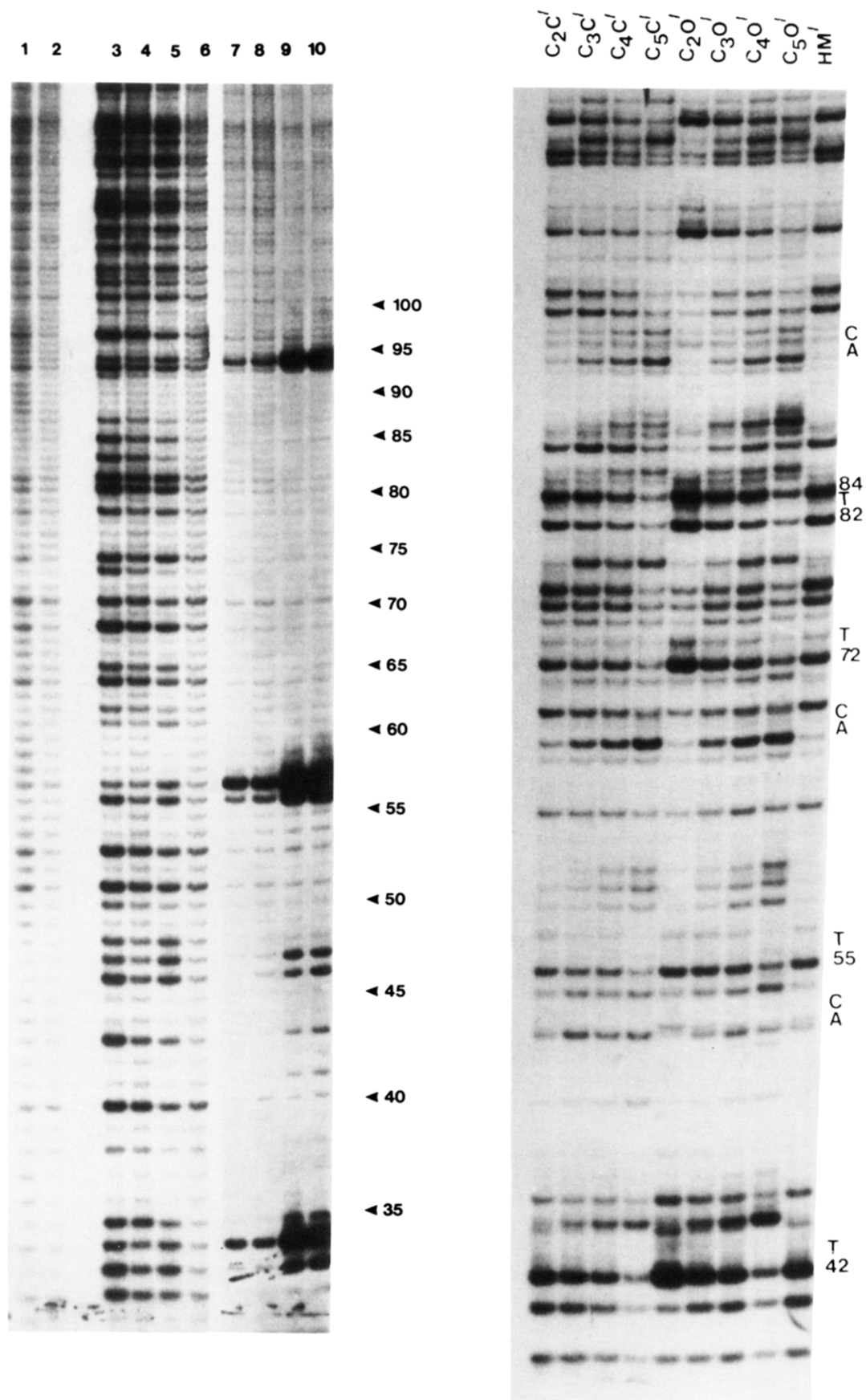
FIGURE 5: (Left panel) Autoradiograph of strand cleavage patterns obtained by using treatment B from 3'-end-labeled DNA incubated with $(CH_2)_4O$, MeO, and CC-1065 in the presence of 30 mM NaCl or 10 mM $MgCl_2$. Lane numbers correspond to DNA control, $(CH_2)_4O$ (d/bp = 0.02), MeO (d/bp = 0.40), CC-1065 (d/bp – 0.0002), and CC-1065 (d/bp = 0.002) in the presence of NaCl (lanes 1, 3, 5, 7, and 9) and in the presence of $MgCl_2$ (lanes 2, 4, 6, 8, and 10), respectively. (Right panel) Autoradiograph of strand cleavage patterns obtained by using treatment B for 5'-end-labeled DNA incubated with the homologous series $(CH_2)_n$ (designated $C_nC$) or the series $(CH_2)_nO$ (designated $C_nO$). Numbers correspond to the guanine positions in the pBR322 fragment.
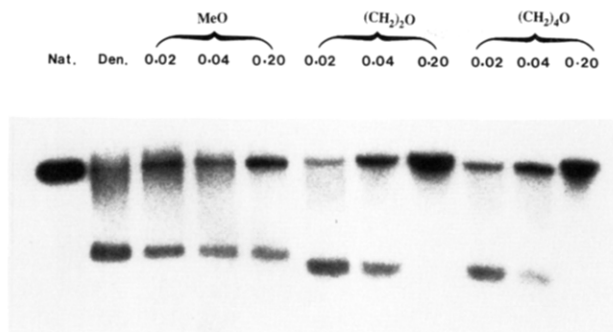
FIGURE 6: Autoradiograph obtained from cross-linking experiments using 3'-end-labeled *Eco*RI digested linear pBR322 incubated at three different drug to base pair ratios (0.02, 0.04, and 0.20) with the compounds MeO, $(CH_2)_2O$, and $(CH_2)_4O$.
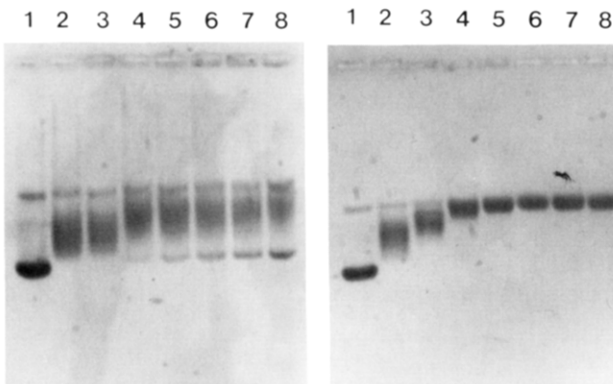


FIGURE 7: Results of unwinding of closed circular superhelical plasmid pBR322 in the presence of $(CH_2)_2$ (left) and $(CH_2)_4O$ (right) at drug to base pair ratios 0.00, 0.10, 0.15, 0.20, 0.25, 0.30, 0.35, and 0.40 (numbered 1–8 in the figure).



FIGURE 8: Plots of percent change of MEP at $N^3$ of adenine (top) and $N^7$ of adenine (bottom) (see text for details). The middle lane is a densitometer scan obtained from the autoradiograph for $(CH_2)_6$ with the guanine peaks omitted.



FIGURE 9: Schematic view into the major groove of the most preferred sequence 5'-GTA. The shaded rectangle represents the 9-amino-acridine chromophore in an intercalated position. The two arrows represent the bifunctional mustard group. The two possible alkylation sites, the $N^7$ of purines, are shown in circles.

drawn regarding the sequence selectivity of alkylation shown by these drugs.

First, compound $(CH_2)_2S$ requires thymine and purine bases to the 3'-side of the guanine which is alkylated. This is true also (but to a lesser extent) with compound $(CH_2)_2O$, whereas $(CH_2)_3$ does not show such sequence selectivity. This requirement for sulfur or oxygen as the para substituent to observe the 5'-GT selectivity suggests that there exists some sort of stereoelectronic interaction between these elements and the DNA major groove. The differences observed between the carbon and the oxygen series in the superhelix unwinding experiments are consistent with the idea that the DNA complexes of the compounds of these two series are conformationally different in some way.

Second, the lack of specificity on the 5'-side strongly implies that the intercalation is occurring between these bases adjacent to the alkylation site. A similar conclusion was drawn by Kohn et al. (1987) to explain the alkylation pattern of quinacrine mustard. The preference of such sequences for intercalation is not surprising, since 9-aminoacridine shows a preference for intercalating at py3'–5'pu base steps (Neidle & Abraham, 1984). Intercalation between cytosine and purine in the sequence 5'-GCPu is also preferred by the 9-aminoacridine chromophore. However, the amino group of cytosine situated directly under the $N^7$ of guanine enables it to exert an electrostatic effect, reducing its nucleophilicity and hence its reactivity. In fact, the 5'-GC dinucleotide sequence is the least preferred site for many alkylating agents (Kohn et al., 1987).

The third point is that as the chain length is increased from three to six atoms in total, there is a switch from guanine alkylation in 5'-GT sequences to adenine alkylation in the complementary 5'-AC sequence. This is strong, if indirect,
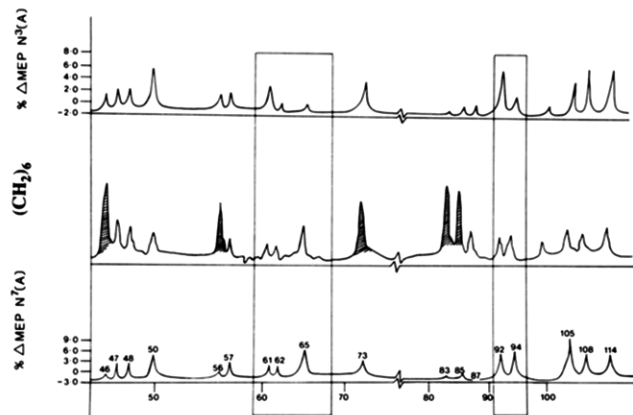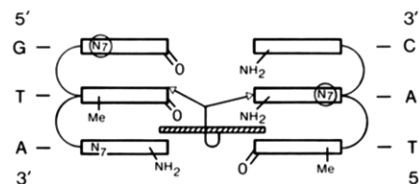
evidence that the alkylation of purines at these complementary sequences is occurring from the same side of DNA. It is well established that guanine alkylation by nitrogen mustards occurs at $N^7$ in the major groove of the DNA helix (Mattes et al., 1986). Therefore, the adenine alkylation seen here must also be occurring in the major groove, more specifically at $N^7$ of adenine. This conclusion is contrary to the current belief that adenine alkylation takes place at the more nucleophilic $N^3$ site of adenine in the minor groove (Grunberg & Haseltine, 1980). In the past decade, quantum mechanical methods have been developed (Perahia & Pullman, 1979) to evaluate the nucleophilicity of different sites in DNA. The molecular electrostatic potential (MEP), and hence nucleophilicity, at $N^7$ and $N^3$ sites of adenine is enhanced when the base is incorporated within the DNA structure and can be significantly affected by neighboring base sequences. For $N^7$ and $N^3$ of adenine, plots of percent change in MEP (kilocalories per mole) of an adenine sandwiched in any triplet sequence, NpApN, occurring in the 375 base pair fragment used in this work from that of an isolated adenine are shown in Figure 8, along with a densitometer scan for alkylation by compound $(CH_2)_6$. For convenience and ease of comparison, only the adenine bands are shown for $(CH_2)_6$. It is clear from both the $N^7$ and $N^3$ plots that the adenines in 5'-AC sequences are not predicted by this calculation to be strong alkylation sites. Thus, the levels of alkylation at AC sequences observed for $(CH_2)_6$ and other long side chain molecules must be related to the influence of the intercalating chromophore. It can also be seen from Figure 8 that the pattern of alkylation of adenines from sequences other than 5'-AC resembles more closely the $N^7$ MEP plot rather than the $N^3$ plot (boxed areas in the figure). This is further evidence for alkylation at the $N^7$ of adenine.

A schematic representation of drug binding to the 5'-GTA sequence in the major groove is shown in Figure 9. A similar

model was proposed for the alkylation of DNA by quinacrine mustard (Kohn et al., 1987). By use of CPK models to identify structural constraints within the complexes of the acridine compounds with DNA, it was concluded that short side chains (3–4 atoms total) confer a degree of rigidity to the molecule, orienting the aniline mustard group approximately at right angles to the 9-aminoacridine plane and giving it the appropriate configuration for interaction with $N^7$ of guanine. The short side chain is not flexible enough to fold back on itself to reach $N^7$ of adenine when the chromophore is intercalated between the thymine and purine bases. When oxygen or sulfur atoms are present in the linker chain, as in compounds (C-$H_2)_2O$ and $(CH_2)_2S$, they can be involved in hydrogen-bonding interactions in the major groove, leading to enhanced reactivity of guanine at $N^7$ in the 5'-GT sequence. However, when the chain length is increased, contraints on the backbone flexibility are removed, facilitating alkylation at the $N^7$ of adenine irrespective of the nature of the link group present.

The quinazoline derivative $Q(CH_2)_3$ shows a different pattern of adenine alkylation, although its pattern of guanine alkylation is similar to that of the corresponding 9-aminoacridine derivative $(CH_2)_3$. It is difficult to explain its preference for adenines in some 5'-AC sequences and not others. The quinazoline moiety is not a strong intercalator, but it may bind weakly from the major groove side, facilitating alkylation at $N^7$ of adenine. In contrast, $B(CH_2)_3$, with a sterically hindered chromophore, shows an overall decrease in DNA alkylation ability and a marked preference for alkylating guanines in 5'-GT and Gn sequences, compared with the parent compound $(CH_2)_3$. Quinacrine mustard, which also shows preference for such sequences (Kohn et al., 1987), has methoxy and chloro groups on the intercalating chromophore which, while not as bulky as *tert*-butyl, can limit the chromophore's freedom to bind via intercalation. These results indicate that the presence of such groups can inhibit intercalation at sites where 9-aminoacridine has only a weak preference for binding. Thus, we observe markedly decreased alkylation of isolated guanines occurring in weak intercalating sites, but only moderate decreases at the strong intercalating 5'-GT sequence. On the other hand, alkylation of guanine occurring in runs of guanines is not greatly affected, since guanines exhibit strong nucleophilic character when occurring in clusters (Kohn et al., 1987). In comparison, the three untargeted mustards Me, MeO, and MeS showed identical alkylation patterns. All guanines were alkylated with equal intensity, although sequence-selective alkylation of adenine was observed in runs of adenines and in 5'-TTA sequences.

The finding that adenine alkylation by compounds $(CH_2)_4O$ and MeO is selectively suppressed by the divalent cation $Mg^{2+}$ is also rather unexpected. This effect is not observed for CC-1065, which alkylates DNA at the $N^3$ of adenine. The ratio of $[Mg^{2+}]$ to $[PO_4^-]$ in the present studies is 10 mM:30 $\mu M$ (i.e., 333:1). Only negligible inhibitory effects on the alkylation patterns of the mustards were seen at $[Mg^{2+}]$ below 1 mM. At such a high ratio, magnesium could possibly either bind to DNA in a site-specific manner or alternatively change the structure so as to modify the accessibility and/or reactivity at some of the binding sites. Although $Mg^{2+}$ is thought to interact with the negative phosphate backbone of DNA through nonspecific electrostatic interactions (Porschke, 1976), many reports in the literature indicate that $Mg^{2+}$ alters the binding of ligands to DNA in ways not observed for monovalent ions of similar or higher ionic strengths (Rose et al., 1980; Granot et al., 1982; Porschke, 1979; Prive et al., 1987). The strongest evidence for specific magnesium binding to DNA

comes from $^{25}Mg$ NMR studies (Rose et al., 1980), where site-specific binding dominates over nonspecific binding. These results suggest that at high concentrations divalent cations bind to DNA bases directly in a site-specific manner.

Thus, the observed inhibition of alkylation at certain DNA sites by the drugs under investigation in the presence of high concentrations of $Mg^{2+}$ could be due to either binding of the divalent cation to DNA in a site-specific manner or its alteration of DNA structure. The finding that $Mg^{2+}$ suppresses the alkylation of adenine by compounds $(CH_2)_4O$ and MeO but not that of CC-1065 indicates that the adenine alkylation site for the mustards is $N^7$ rather than $N^3$, consistent with the conclusions based on GT/AC selectivity.

This observation that $Mg^{2+}$ ions may alter the base selectivity of alkylation of DNA by these compounds has implications for correlating in vitro data for alkylators with the way in which they may interact with DNA under in vivo conditions. The $[Mg^{2+}]$ in mammalian cells in vivo is in the millimolar range (Eichhorn et al., 1980), and it has been shown by electron microscopy that the nature of chromatin packing in the cell nucleus is dependent upon $[Mg^{2+}]$ (Monneron & Moule, 1968; Hogan et al., 1986). Our results show that it may be important to consider the effects of divalent metal ions at physiological concentrations in studies of alkylator–DNA interactions. The $[Mg^{2+}]$ effect may also prove useful elsewhere in helping to distinguish between alkylation at $N^7$ and alkylation at $N^3$ sites in adenine.

The kinetics of DNA alkylation indicate that, for all the compounds studied, the majority of the drug is hydrolyzed and only a small fraction gives rise to DNA adducts. This may be due to the catalytic effect of DNA on drug hydrolysis. It is well-known that DNA catalyzes the hydrolysis of the diol epoxides of polycyclic hydrocarbons, through stabilization of a carbonium ion intermediate (Geacintov et al., 1984). A similar situation may occur in the case of aniline mustards, where reaction proceeds via an intermediate aziridinium ion. The acridine-linked mustards remain intercalated even after alkylation, as indicated by the superhelix unwinding experiments. However, differences in the conformations of the DNA–drug covalent complexes, which depend on the side-chain structure, are revealed by the unwinding results obtained for compounds $(CH_2)_4O$ and $(CH_2)_3$ (Figure 7). The inability of the compounds of the oxygen series to induce reverse superhelical turns suggests some form of stereoelectronic interaction between the oxygen atom and DNA that limits rewinding of the superhelix.

The overall reactivity of the three homologous series of compounds studied here, $(CH_2)_n$, $(CH_2)_nO$, and $(CH_2)_nS$, is controlled primarily by the electronic properties of the para substituent on the mustard (Hammett $\sigma_p$ values −0.27, −0.17, and 0.0, respectively), as noted previously (Gourdie et al., 1990). In studies of a fourth series of compounds $[(CH_2)_nSO_2]$ we were unable to detect any DNA adducts under the experimental conditions employed, due to the much lesser reactivity of these mustards ($\sigma_p$ 0.72). However, within each class the DNA-targeted acridine-linked mustards alkylate DNA much more readily than the corresponding untargeted mustards, as illustrated by the difference in drug to base pair ratios required for the compounds to cause similar levels of DNA breakage following chemical treatment in the gel experiments. These results parallel the relative in vitro cytotoxicities ($IC_{50}$ values) of the compounds against P388 leukemia cells, where the $(CH_2)_nO$ and $(CH_2)_n$ compounds are much more cytotoxic than the $(CH_2)_nS$ series, with the $(CH_2)_nSO_2$ series being least potent. In addition, within each

series the acridine-linked mustards show higher cytotoxicity than the corresponding untargeted mustards (Gourdie et al., 1990; Valu et al., 1990). The $(CH_2)_nS$ compounds also show much lower cross-linking capabilities than the compounds in the $(CH_2)_nO$ and $(CH_2)_n$ series. This is consistent with the results from comparative cell line studies using AA8 cells and the UV4 subline of AA8. The latter cells lack the ability to perform the incision step of excision repair of DNA lesions (Thompson et al., 1980) and thus are hypersensitive to DNA adducts, in particular cross-links. Ratios of the $IC_{50}$ values in the two cell lines [the hypersensitivity factor, $HF = IC_{50}$-$(AA8)/IC_{50}(UV4)]$ of $>20$ suggest that DNA cross-linking is the major mechanism of cytotoxicity (Wilson et al., 1989). Compounds in the $(CH_2)_nO$ and $(CH_2)_n$ series show much higher HFs (ca. 40) than those in the $(CH_2)_nS$ series (ca. 10), while compounds in the $(CH_2)_nSO_2$ series have HFs of ca. 1, suggesting they do not act by DNA adduct formation at all (Valu et al., 1990).

The in vivo antitumor activities of these compounds have also been evaluated (Gourdie et al., 1990; Valu et al., 1990). The $(CH_2)_nO$ and $(CH_2)_n$ compounds show higher activity (ILS values of 50–60%) and much greater potency (optimal doses of 20–30 mg/kg) than either chlorambucil (ILS 33% at an optimal dose of 225 mg/kg) or any of the untargeted mustards, using a single-dose protocol. In contrast, compounds in the $(CH_2)_nS$ and $(CH_2)_nSO_2$ series showed only minimal in vivo activity. Thus, clear relationships appear to exist between drug structure, mustard group reactivity, overall DNA alkylation, DNA cross-linking abilities, and in vivo antitumor activity.

In contrast, while there are relationships between drug structure and both the site and sequence selectivity of alkylation by the acridine-linked mustards, there appear to be no obvious relationships between these properties and the simple measures of in vivo activity studied so far. The compounds also show low level of cross-linking compared to overall DNA alkylation, on average one interstrand cross-link from about 20 alkylation events per 4362 base pair length of DNA for compounds in the $(CH_2)_nO$ and $(CH_2)_n$ series and even lower levels for the $C_nS$ series. Thus, there has been little improvement in the monoadduct to cross-linking ratio over that estimated previously for untargeted mustards (Brendel & Ruhland, 1984). This is disappointing from a drug design point of view, since monoadduct events are liable to be more genotoxic and mutagenic rather than cytotoxic (Brendel & Ruhland, 1984), and the need is to maximize *both* the overall extent of DNA alkylation *and* the ratio of monoadduct to cross-linking events.

## SUPPLEMENTARY MATERIAL AVAILABLE

Detailed syntheses of compounds $B(CH_2)_3$, $Q(CH_2)_3$, and $HM(CH_2)_3$ (2 pages). Ordering information is given on any current masthead page.

## REFERENCES

Brendel, M., & Ruhland, A. (1984) *Mutat. Res. 133*, 51–85.

Eichhorn, G. L., Butzow, J. J., Clark, P., Von Hahn, H. P., Rao, G., Heim, J. M., Tarien, E., Crapper, D. R., & Karlik, S. J. (1980) *Inorganic Chemistry in Biology and Medicine*, (Martel, A. E., Ed.) ACS Symposium Series 140, pp 75–88, American Chemical Society, Washington, DC.

Garcia, S. T., McQuillan, A., & Panasci, L. (1988) *Biochem. Pharmacol. 37*, 3189–3192.

Geacintov, N. E., Hibshoosh, H., Ibanez, V., Benjamin, M. J., & Harvey, R. G. (1984) *Biophys. Chem. 20*, 121–133.

Gourdie, T. A., Valu, K. K., Gravatt, G. L., Boritzki, T. J., Baguley, B. C., Wilson, W. R., Woodgate, P. D., & Denny, W. A. (1990) *J. Med. Chem. 33*, 1177–1186.

Granot, J., Feigon, J., & Kearns, D. R. (1982) *Biopolymers 21*, 181–201.

Grunberg, S. M., & Haseltine, W. A. (1980) *Proc. Natl. Acad. Sci. U.S.A. 77*, 6546–6550.

Hogan, M. E., Hayes, B., & Wang, N. C. (1986) *Biochemistry 25*, 5070–5082.

Hurley, L. H., Lee, C. S., McGovren, J. P., Warpehoski, M. A., Mitchell, M. A., Kelly, R. C., & Aristoff, P. A. (1988) *Biochemistry 27*, 3886–3892.

Kohn, K. W., Hartley, J. A., & Mattes, W. B. (1987) *Nucleic Acids Res. 15*, 10531–10549.

Mattes, W. B., Hartley, J. A., & Kohn, K. W. (1986) *Nucleic Acids Res. 14*, 2971–2987.

Maxam, A. M., & Gilbert, W. (1977) *Proc. Natl. Acad. Sci. U.S.A. 74*, 560–564.

Maxam, A. M., & Gilbert, W. (1980) *Methods Enzymol. 65*, 499–560.

Monneron, A., & Moule, Y. (1968) *Exp. Cell Res. 51*, 531–537.

Neidle, S., & Abraham, Z. (1984) *CRC Crit. Rev. Biochem. 17*, 73–121.

Perahia, D., & Pullman, A. (1979) *Theor. Chim. Acta 50*, 351–354.

Porschke, D. (1976) *Biophys. Chem. 4*, 383–391.

Porschke, D. (1979) *Nucleic Acids Res. 6*, 883–898.

Price, C. C., Gaucher, G. M., Koneru, P., Shibikawa, R., Sowa, J. R., & Yamaguchi, M. (1968) *Biochim. Biophys. Acta 166*, 327–334.

Prive, G. G., Heinemann, U., Chandrasegaran, S., Kan, L-S, Kopka, M. L., & Dickerson, R. E. (1987) *Science 238*, 498–504.

Roberts, J. J. (1978) *Adv. Radiat. Biol. 7*, 5211–5217.

Rose, D. M., Bleam, M. L., Record, M. T., Jr., & Bryan, R. G. (1980) *Proc. Natl. Acad. Sci. U.S.A. 77*, 6289–6292.

Ross, W. C. J. (1949) *J. Chem. Soc.*, 183–191.

Suzukake, K., Vistica, B. P., & Vistica, D. T. (1983) *Biochem. Pharmacol. 32*, 165–167.

Thompson, L. H., Busch, D. B., Brookman, K., Mooney, C. L., & Glaser, D. A. (1981) *Proc. Natl. Acad. Sci. U.S.A. 78*, 3734–3737.

Valu, K. K., Gourdie, T. A., Boritzki, T. J., Gravatt, G. L., Baguley, B. C., Wilson, W. R., Woodgate, P. D., & Denny, W. A. (1990) *J. Med. Chem.* (in press).

Wang, A. L., & Tew, K. D. (1985) *Cancer Treat. Rep. 69*, 677–682.

Wilson, W. R., Thompson, L. H., Anderson, R. F., & Denny, W. A. (1989) *J. Med. Chem. 32*, 31–38.

Young, C. W., Yagoda, A., Bittar, E. S., Smith, S. W., Grabstald, H., & Whitmore, W. (1976) *Cancer 38*, 1887–1895.